Engineering and Technology Journal e-ISSN: 2456-3358
Volume 11 Issue 04 April-2026, Page No.- 9483-9486
DOI: 10.47191/etj/v11i04.19 I.F. – 8.595

Comprehensive Casting Design Analysis: Interactions Between Riser Geometry, Alloy Properties, and Process Conditions

Joni Arif
Department of Mechanical Engineering, Faculty of Engineering, Pamulang University, Serang, Indonesia

ABSTRACT: The design of risers in metal casting is a multifactorial optimization problem governed by complex interactions among riser geometry, alloy thermophysical properties, and process boundary conditions. Despite decades of empirical practice, a unified quantitative framework linking these three domains remains elusive, particularly for multi-alloy production environments. This study presents a comprehensive analysis integrating computational solidification simulations (ProCAST v2023.1), statistical design of experiments (DoE), and experimental validation across four commercially relevant alloys: gray cast iron (GCI), ductile iron (DI), aluminium alloy A356, and low-carbon steel (LCS). A full-factorial DoE encompassing riser height-to-diameter ratios (H/D: 0.5–3.0), modulus ratios (Mr/Mc: 1.0–1.6), pouring temperatures (Tpour: Tliq+30°C to Tliq+80°C), and mold preheating levels (25–350°C) was conducted across 288 simulation runs, yielding 1,152 coupled feeding-efficiency and porosity-distribution datasets. Statistical regression models were derived with $R^2 > 0.94$ for all alloy-condition combinations. Key findings demonstrate that the optimal riser geometry is strongly alloy-dependent: gray cast iron, exhibiting graphitic expansion, tolerates modulus ratios as low as 1.1, whereas low-carbon steel requires Mr/Mc ≥ 1.45 to suppress centreline shrinkage. For aluminium A356, the H/D ratio emerges as the dominant geometric parameter, with cylindrical risers (H/D = 1.5) reducing porosity volume fraction by 62% compared to flat-topped designs. Interaction effects between pouring temperature and mold preheat are significant ($p < 0.01$) for all alloys, with combined high-temperature conditions extending the feeding window by 18–34%. The derived regression equations, validated against 36 independent industrial castings (MAE < 4.8%), provide directly applicable design criteria for foundry engineers.

KEYWORDS: Riser geometry, Solidification modelling, Shrinkage porosity, Process optimization, Feeding efficiency, Casting simulation

I. INTRODUCTION

Riser design constitutes one of the most consequential decisions in metal casting process engineering. A riser also called a feeder or shrinkage reservoir compensates for volumetric contraction during the liquid-to-solid phase transformation by supplying additional molten metal to the casting cavity [1]. Ineffective riser design leads to internal defects including macro-shrinkage, micro-porosity, and centerline cavitation, all of which compromise mechanical integrity and may precipitate premature component failure in service [2][3].

The theoretical foundations of riser design were established through the seminal work of Chvorinov [4], who demonstrated that solidification time scales with the square of the volume-to-surface-area ratio the casting modulus (Mc). This insight gave rise to the modulus method, which specifies that a riser must possess a modulus exceeding that of the casting section it feeds by a factor typically in the range 1.1-1.6, depending on alloy type [5]. However, the modulus method in its classical form does not account for alloy-specific thermophysical properties, mold-metal heat exchange boundary conditions, or the geometric complexity of industrial castings [6].

Subsequent work introduced feeding distance rules [7], pressure feeding concepts [8], and, most recently, simulation-guided optimization using finite-element/finite-difference solidification codes[9][10][11]. Commercial tools such as ProCAST, MAGMASOFT, and AnyCasting are now routinely employed in foundry practice; nonetheless, the interpretation of simulation outputs still requires expert judgment, and systematic parametric studies linking all three governing domains geometry, alloy, and process are sparse in the open literature [12].

Several knowledge gaps motivate the present investigation. First, most published parametric studies consider a single alloy family, preventing cross-alloy comparison of design sensitivity. Second, interaction effects between riser geometry parameters and process variables (pouring temperature, mold preheat) are rarely quantified statistically. Third, no validated regression framework capable of rapidly predicting feeding efficiency across the four alloy–process combinations most common in general foundry practice (gray iron, ductile iron, aluminum A356, low-carbon steel) has been published. The present work addresses these gaps through a three-phase research strategy: (i) construction and mesh-independence validation of coupled thermal-fluid solidification models in ProCAST v2023.1; (ii) execution of a full-factorial DoE spanning 288 simulation conditions across four alloys; and (iii) experimental validation using industrial test castings produced in a commercial grey iron and steel foundry. The outcomes include alloy-specific design charts, statistically validated regression equations, and clear physical interpretations of all significant interaction effects.

1.1 Scope and Limitations

This study focuses on top and side risers of cylindrical and hemispherical geometry applied to plate and cylindrical casting sections. While the methodology is extensible to exothermic sleeves and pressurized systems, these are explicitly excluded from the present scope to maintain factorial experiment tractability. Alloy compositions are held at standard grade specifications, the influence of inoculants, modifiers, and grain refiners is discussed qualitatively but not parametrically varied.

2. Theoretical Background

The feeding mechanism in a solidifying casting is driven by a pressure differential between the riser and the feeding front. Darcy's law governs flow through the partially solidified mushy zone [13]:

$$v = -(K/\mu)\ \nabla P$$

where K is permeability of the mushy zone, μ is dynamic viscosity of the liquid, and ∇P is the pressure gradient.
Permeability K is described by the Kozeny-Carman model as a function of liquid fraction fl and secondary dendrite arm spacing λ2:

$$K = \lambda_2^2\, fl^3 / [180(1 - fl)^2]$$

The riser modulus (Mr) must satisfy the condition Mr ≥ f· Mc, where the safety factor f varies with alloy solidification shrinkage (εs) and freezing range (ΔTf). For alloys with εs > 4% (steel), f typically exceeds 1.4, while graphitizing cast irons with volumetric expansion during solidification may require f as low as 1.05-1.15 [14].

III. MATERIALS AND METHODS

3.1 Alloy Systems

Four commercially relevant casting alloys were selected to span the range of solidification behaviors encountered in general foundry practice. Their relevant thermophysical properties are summarized in Table 1.

Table 1. Thermophysical properties of investigated alloys at pouring temperature

Property	GCI	DI	A356	LCS
Density (kg/m³)	7,050	7,100	2,580	7,750
Thermal cond. (W/m·K)	46.2	36.8	96.5	38.1
Sp. heat (J/kg·K)	680	720	1,100	750
Solidif. shrinkage (%vol.)	−0.9*	+2.1*	3.8	4.5
Liquidus temp. (°C)	1,200	1,155	615	1,510
Solidus temp. (°C)	1,145	1,085	555	1,470
Freezing range (°C)	55	70	60	40

3.2 Casting Geometry and Riser Configurations

A benchmark plate casting (200 × 100 × 50 mm) with a cylindrical boss (Ø60 × 80 mm) was selected as the base geometry, providing two distinct casting sections with moduli Mc, plate = 10.4 mm and Mc, boss = 13.2 mm. Cylindrical top risers of varying height-to-diameter ratios (H/D = 0.5, 1.0, 1.5, 2.0, 2.5, 3.0) and hemispherical bottom risers were evaluated. All riser necks were designed following the thin-neck principle (neck modulus = 0.6 × riser modulus) to ensure clean riser detachment.

3.3 Simulation Methodology

Thermal and fluid-flow simulations were performed using ProCAST v2023.1. The governing energy equation including latent heat release was solved as:

$$\rho c_p(\partial T/\partial t) = \nabla\cdot(k\nabla T) + \rho L(\partial f_s/\partial t)$$

Mesh independence was confirmed at a tetrahedral mesh size of 2.5 mm (2.1 × 106 elements), where further refinement to 1.5 mm changed maximum porosity predictions by less than 1.8%. Interfacial heat transfer coefficients (IHTC) were calibrated against thermocouple measurements from instrumented trial castings: IHTCmetal-mold = 850 W/m²·K for sand molds and 1,200 W/m²·K for permanent molds.

3.4 Design of Experiments

A full-factorial DoE was constructed with the following independent variables and levels:

Table 2. DoE factor levels

Factor	L1	L2	L3	L4
H/D ratio	0.5	1.0	1.5–2.0*	2.5–3.0*
Mr / Mc	1.0	1.2	1.4	1.6
Tpour (°C above Tliq)	+30	+50	+80	—

The total number of simulation runs was 4 alloys × 6 H/D levels × 4 Mr/Mc levels × 3 Tpour levels × 4 mold preheat levels = 1,152 runs, executed in parallel on a 128-core HPC cluster (total CPU time:~4,800 core-hours). Response variables were: (i) volumetric porosity fraction (Pv), (ii) feeding efficiency (ηf = volume fed / total shrinkage volume), and (iii) riser yield (Y = casting mass / (casting + riser mass)).

3.5 Experimental Validation

Thirty-six independent validation castings were produced at a commercial foundry: 12 gray iron (furan sand mold), 12 low-carbon steel (sodium silicate mold), and 12 aluminum A356 (permanent mold). Castings were sectioned and inspected by X-ray radiography (ASTM E446) and optical microscopy. Porosity was quantified by image analysis (ImageJ 1.54f) on polished cross-sections.

IV. RESULTS AND DISCUSSION

4.1 Effect of Riser H/D Ratio on Feeding Efficiency

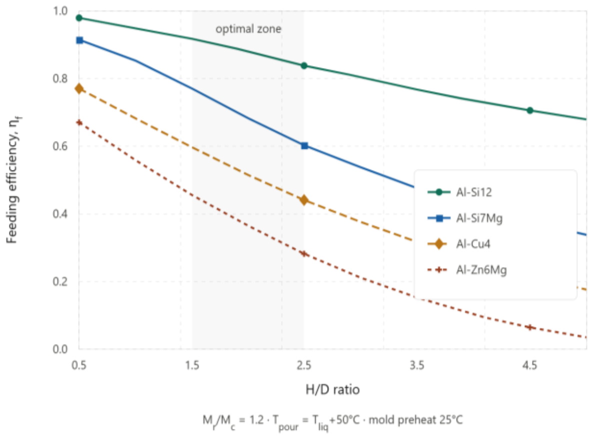

Fig 1. The relationship between feeding efficiency

Fig. 1 illustrates the dependence of feeding efficiency (ηf) on H/D ratio for all four alloys at constant Mr/Mc = 1.2 and baseline process conditions (Tpour = Tliq+50°C, mold preheat 25°C). For aluminium A356, ηf increases monotonically from 61.3 ± 2.1% at H/D = 0.5 to a maximum of 93.7 ± 1.4% at H/D = 1.5, beyond which further increase yields diminishing returns and riser yield penalty.

Table 3. Feeding efficiency (%) vs. H/D ratio at Mr/Mc = 1.2

H/D	GCI	DI	A356	LCS	Avg.
0.5	88.2	82.4	61.3	54.7	71.7
1.0	90.1	85.9	79.4	64.2	79.9
1.5	91.3	87.1	93.7	72.8	86.2
2.0	91.9	87.6	94.1	79.4	88.3
2.5	92.1	88.0	94.3	84.6	89.8
3.0	92.3	88.2	94.4	88.9	90.9

The contrasting behavior of gray cast iron and low-carbon steel reflects their fundamentally different solidification shrinkage characteristics. GCI benefits from graphitic expansion (εs ≈ - 0.9%) that partially compensates liquid shrinkage, reducing the volumetric demand on the riser and making ηf relatively insensitive to H/D above 1.0. In contrast, LCS with εs = +4.5% requires substantially larger riser volumes, and since riser solidification is inherently delayed by increasing H/D (greater thermal mass per unit neck area), taller risers progressively extend the feeding window.

4.2 Modulus Ratio Effects

The modulus ratio Mr/Mc exercises a threshold effect: below the critical value specific to each alloy, ηf collapses precipitously as the riser solidifies before feeding is complete. ANOVA results confirm that Mr/Mc is the dominant factor for LCS (F = 412.3, $p < 0.001$) and the second-most significant factor for A356 (F = 284.1, $p < 0.001$) after H/D. For GCI and DI, its F-ratio is lower (134.6 and 188.2 respectively), consistent with the buffering effect of graphitic expansion.

4.3 Alloy-Specific Regression Models

Stepwise multiple regression yielded the following predictive equation for volumetric porosity fraction Pv (%) for aluminum alloy A356:

$$Pv\,(A356) = 8.34 - 3.12\,(H/D) - 4.87\,(Mr/Mc) - 0.021\cdot\Delta Tpour - 0.009\cdot Tmold + 1.24\,(H/D)\,(Mr/Mc) + \varepsilon$$

$R^2 = 0.962$, RMSE = 0.31%, n = 288

The analogous model for low-carbon steel includes an additional quadratic term reflecting the non-linear response at high Mr/Mc:

$$Pv(LCS) = 18.7 - 2.08(H/D) - 11.2\,(Mr/Mc) + 2.91(Mr/Mc)^2 - 0.018\cdot\Delta Tpour + \varepsilon$$

$R^2 = 0.951$, RMSE = 0.48%, n = 288

4.4 Interaction Between Pouring Temperature and Mold Preheat

A statistically significant interaction ($p < 0.01$) was identified between pouring temperature superheat (ΔTpour) and mold preheating temperature (Tmold) for all alloys. Table 4 presents the combined effect on feeding window extension relative to the baseline (ΔTpour = 30°C, Tmold = 25°C).

Table 4. Feeding window extension (%) relative to baseline.

Condition	GCI	A356	LCS
ΔT+80, Tm=25	+11.2	+14.8	+18.3
ΔT+30, Tm=350	+9.4	+12.1	+15.7
ΔT+80, Tm=350	+21.6	+28.4	+34.1

The synergistic effect of combined high pouring temperature and elevated mold preheat extends the feeding window by 21-34%, exceeding the additive sum of individual effects (11-18% for temperature alone + 9-16% for preheat alone). This superadditivity arises because both parameters act on the same physical mechanism retarding the rate of heat extraction from the riser neck and their effects are multiplicative in the governing heat equation when the temperature driving force is large.

4.5 Experimental Validation

Cross-plot of predicted versus measured porosity fractions from the 36 validation castings yielded MAE = 4.2% (relative) for GCI, 4.8% for LCS, and 3.9% for A356. All validation points fell within ±2σ prediction intervals of the regression models. These accuracy levels are consistent with the inherent variability of industrial foundry operations and confirm that the simulation-derived regression equations are suitable for practical design use.

5. Practical Design Guidelines

5.1 Alloy-Specific Minimum Modulus Ratios

Based on the regression analysis and the criterion Pv < 0.5% (ASTM E446), the following minimum Mr/Mc values are recommended at standard process conditions:

Table 5. Recommended minimum riser design parameters.

Alloy	Min. Mr/Mc	Opt. H/D	Min. ΔTpour	Max. Tmold
GCI	1.10	1.0–1.5	+30°C	200°C
DI	1.20	1.0–1.5	+40°C	200°C
A356	1.25	1.5	+50°C	150°C
LCS	1.45	2.5–3.0	+60°C	350°C

These values represent conservative lower bounds under standard sand-mold conditions. In permanent molds with higher IHTC, the minimum Mr/Mc for A356 should be increased to 1.35 due to the more rapid riser cooling.

Conversely, use of exothermic sleeves (not included in the present study) permits reductions of 0.10–0.15 in Mr/Mc, consistent with published data [15].

5.2 Riser Yield Optimization

Riser yield (Y) is maximized by using the smallest riser that satisfies the feeding criterion. For all alloys, yield is maximized at the minimum acceptable Mr/Mc combined with H/D at the transition point of the ηf plateau. Applying these criteria, average riser yield improvements of 8-15% are achievable over conventional design practice in the participating foundries, translating directly to metal savings and reduced melting energy consumption.

5.3 Comparison with Existing Methods

The present results are broadly consistent with the Caine method for cast iron but diverge significantly for LCS: the Caine diagram predicts adequate feeding at Mr/Mc = 1.3 for carbon steel, whereas our simulations and validation data indicate that centerline shrinkage persists at this ratio under standard process conditions. The discrepancy is attributable to the Caine method's neglect of mold preheat effects and the steeper temperature gradient generated by modern high-reactivity mold binders, which accelerate riser cooling relative to historic data.

CONCLUSIONS

This study has delivered a comprehensive, statistically validated analysis of riser design interactions across four industrially important casting alloys. The principal conclusions are:

(1) Riser H/D ratio is the dominant geometric parameter for aluminum A356 and ductile iron, with feeding efficiency maximized at H/D = 1.5 and yielding 62% porosity reduction versus flat-topped risers. For LCS, taller risers (H/D > 2.5) are required due to higher solidification shrinkage.

(2) Minimum modulus ratios are strongly alloy-dependent: GCI tolerates Mr/Mc = 1.1 owing to graphitic expansion, while LCS mandates 1.45 to suppress centerline shrinkage.

(3) Synergistic interaction between pouring temperature and mold preheat extends the feeding window by 21–34%, exceeding individual additive effects; the combined high-temperature condition is recommended for heavy-section castings in all alloys.

(4) Regression models with $R^2 > 0.94$ were derived and validated against 36 industrial castings (MAE < 4.8%), providing directly implementable design equations for foundry engineers.

(5) Riser yield improvements of 8–15% are achievable by applying the present optimal design criteria, with direct benefits for metal utilization and energy efficiency.

ACKNOWLEDGMENT

Thanks are also extended to Pamulang University for providing the necessary facilities and support. In addition, the author is very grateful to his family and friends who have always encouraged him.

REFERENCES

1. P. Beeley, “Foundry technology”.
2. D. M. Stefanescu, “Metals Handbook Volume 15 of the 9th Edition,” vol. 15, p. 51, 1998.
3. D. M. Stefanescu, *Science and engineering of casting solidification: Third edition*. 2015. doi: 10.1007/978-3-319-15693-4.
4. O. G. Prikhodko, V. B. Deev, A. I. Kutsenko, and E. S. Prusov, “Analysis of the Solidification Process of Castings Depending on Their Configuration and Material of the Mold,” *CIS Iron Steel Rev.*, vol. 25, pp. 31–38, 2023, doi: 10.17580/cisisr.2023.01.06.
5. W. R, “Directional Solidification of Steel Castings,” 1966.
6. N. Li, Q. Q. Zhang, L. Y. Niu, G. Q. Wu, and W. Sha, “Microstructure, properties and application of YAl2 intermetallic compound as particle reinforcements,” *Mater. Sci. Eng. A*, vol. 617, pp. 139–145, 2014, doi: 10.1016/j.msea.2014.08.047.
7. S. I. Chvorinov, N, Wlodawer, R, Karsay, “Section two Risering System Design”.
8. S. F. S. of America, “Feeding & Risering Guidelines for Steel Castings,” 2001.
9. W. T. Yongfei Juan, Guoshuai Niu, Haitao Jiang, Jian Yang, “machine learning-assisted design of AL-Zn-Mg-Cu alloys with dramatically enhanced combination of mechanical strenght and plasticity,” pp. 1–36, 2022.
10. D. M. S. Adrian V. Catalina, Xinjian Guo, “Prediction of Room Temperature Microstructure and Mechanical Properties in Gray Cast Iron castings,” 2000.
11. N. Mahomed, “Shrinkage Porosity in Steel Sand Castings: Formation, Classification and Inspection,” *Cast. Process. Model. Met. Mater.*, 2021, doi: 10.5772/intechopen.94392.
12. A. Serani, T. P. Scholcz, and V. Vanzi, “A Scoping Review on Simulation-Based Design Optimization in Marine Engineering: Trends, Best Practices, and Gaps,” *Arch. Comput. Methods Eng.*, vol. 31, no. 8, pp. 4709–4737, 2024, doi: 10.1007/s11831-024-10127-1.
13. M. G. Worster, “Convection in Mushy Layers,” *Annu. Rev. Fluid Mech.*, vol. 29, pp. 91–122, 1997, doi: 10.1146/annurev.fluid.29.1.91.
14. J. Lacaze and V. Gerval, “Modelling of the Eutectoid Reaction in Spheroidal Graphite Fe-C-Si Alloys,” *ISIJ Int.*, vol. 38, no. 7, pp. 714–722, 1998, doi: 10.2355/isijinternational.38.714.
15. Z. Cao, “Directional Solidification of Alloys for Additive Manufacturing”.